On-Chip Optical Squeezing

Avik Dutt,[1,*] Kevin Luke,[1] Sasikanth Manipatruni,[2] Alexander L. Gaeta,[3,4]
Paulo Nussenzveig,[1,5] and Michal Lipson[1,4]

[1]*School of Electrical and Computer Engineering, Cornell University, Ithaca, New York 14853, USA*
[2]*Exploratory Integrated Circuits, Intel Components Research, Intel Corporation,
Hillsboro, Oregon 97124, USA*
[3]*School of Applied and Engineering Physics, Cornell University, Ithaca, New York 14853, USA*
[4]*Kavli Institute at Cornell for Nanoscale Science, Cornell University, Ithaca, New York 14853, USA*
[5]*Instituto de Física, Universidade de São Paulo, P.O. Box 66318, 05315-970 São Paulo, Brazil*

We report the observation of all-optical squeezing in an on-chip monolithically integrated CMOS-compatible platform. Our device consists of a low-loss silicon nitride microring optical parametric oscillator (OPO) with a gigahertz cavity linewidth. We measure 1.7 dB (5 dB corrected for losses) of sub-shot-noise quantum correlations between bright twin beams generated in the microring four-wave-mixing OPO pumped above threshold. This experiment demonstrates a compact, robust, and scalable platform for quantum-optics and quantum-information experiments on chip.

I. INTRODUCTION

Quantum properties of light can be used in a myriad of applications ranging from enhanced sensing [1,2] to spectroscopy [3,4] to metrology [5,6] and quantum-information processing [7,8]. Especially in the latter case, it is desirable to have nonclassical light sources on compact platforms with a very small footprint, high degree of confinement, low-power operation, and compatibility with complementary-metal-oxide-semiconductor (CMOS) technology. In addition to the possibility of leveraging on a mature fabrication technology that is already in place, such a CMOS-compatible platform will enable the integration of microelectronics with quantum photonics on the same substrate. Many efforts have been directed at the development of on-chip single-photon light sources [9–14], detectors [15], and logic gates [8]. The development of brighter nonclassical light sources, such as squeezed light sources [16], on CMOS-compatible platforms has been lagging behind.

The generation of squeezed states of light requires an optical nonlinearity and was initially demonstrated in several off-chip platforms including optical parametric oscillators (OPOs) using parametric down-conversion [17] and in atomic vapors [18] and optical fibers [19] using four-wave mixing. In such nonlinear parametric processes, two "twin" beams are generated, called signal and idler beams, with strong quantum correlations in the intensities of the two beams, leading to noise in their intensity difference reduced below the standard quantum limit. In order to boost the effective optical nonlinearity, it is customary to use a cavity. This cavity introduces a trade-off between high bandwidth and high squeezing. On the

one hand, the cavity should have a high finesse in order to achieve stronger squeezing. On the other hand, typically a high finesse implies low bandwidth, as is the case in free-space OPOs. But for applications such as entanglement-based quantum key distribution in the continuous-variable regime [20], a large squeezing bandwidth is essential to ensure high data rates. Bright twin-beam intensity-difference squeezing has been recently demonstrated in whispering-gallery-mode crystalline resonators made of lithium niobate [21], but the platform is not integrated on chip and has a cavity bandwidth of 30 MHz. Recently, Ast *et al.* [22] observed broadband squeezing over a gigahertz by using a low-finesse cavity for field enhancement. However, as Ast *et al.* point out [22,23], the consequences are a very high parametric oscillation threshold. Another approach to achieve strong squeezing is to use a pulsed pump in order to achieve very high intensities and, thus, strong nonlinear behavior. Using a periodically poled lithium niobate waveguide, Eto *et al.* [24] measured squeezing of 5 dB. In their work, since there is no cavity, there is no fundamental bandwidth trade-off, the data rate limit being related to the repetition rate of the pulsed pump. However, CMOS compatibility and a high degree of confinement, which are desirable in making compact integrated photonic structures, is lacking. It should be noted that Safavi-Naeini *et al.* [25] have reported 0.2-dB squeezing of light using a silicon optomechanical resonator, which, although CMOS compatible, is intrinsically restricted to a bandwidth of a few megahertz around the mechanical resonance and uses suspended structures operating at low temperatures, making it less robust compared to sources based on all-optical nonlinearities.

In this article, we report the observation of all-optical squeezing in an on-chip monolithically integrated
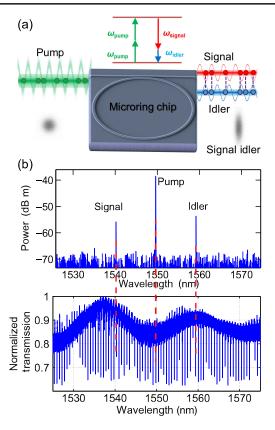
[*]ad654@cornell.edu

FIG. 1.   (a) Schematic of the generation of intensity-correlated signal and idler beams via four-wave mixing in the on-chip microring optical parametric oscillator (OPO). (b) Top: Optical spectrum analyzer scan of the light coupled out of the chip, at a pump power just above the parametric oscillation threshold. The Si_3N_4 ring is pumped at 1549.6 nm, generating signal and idler modes at 1540.2 and 1559.2 nm, respectively, which are 15 cavity modes away from the pump wavelength, as can be seen in the bottom figure. Bottom: Transmission spectrum of the ring for transverse-electric (TE) polarization.

CMOS-compatible platform generated in a micron-size silicon nitride oscillator [26] with gigahertz cavity linewidth. Owing to the small size of on-chip cavities, it is possible to obtain a large finesse and still have relatively wide cavity bandwidths. Large intracavity pump enhancement and strong squeezing can, thus, be obtained. Our OPO is based on the third-order nonlinear process of four-wave mixing (FWM), as shown in Fig. 1. These devices consist of microring resonators fabricated on deposited films of Si_3N_4 (inset of Fig. 2). Note that the OPO can generate, in principle, a very large number of beams spanning more than an octave [27,28]. Here we generate squeezing by using a pump power that is just above the threshold when only two modes oscillate.

II. METHODOLOGY

A. Design

We fabricate the microring resonators out of silicon nitride because of its high nonlinear refractive index [26]
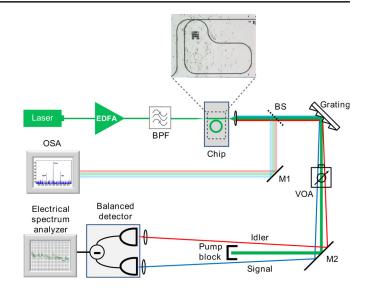

FIG. 2.   Experiment setup. The on-chip microring resonator is pumped by a continuous-wave laser followed by an erbium-doped fiber amplifier (EDFA) from JDS Uniphase and a bandpass filter (BPF). To ensure efficient coupling in and out of the chip, inverse tapers are used [29]. A lensed fiber is used for input coupling. The output from the waveguide is collected with a high-NA objective lens. The diffraction grating spatially separates the pump and the twin beams. After blocking the pump, the beams are focused on a balanced detector. The rf output of the balanced detector is sent to an electrical spectrum analyzer. A small fraction of the beams is sent to an optical spectrum analyzer (OSA) to monitor the onset of parametric oscillation. The inset shows a microscope image of the ring resonator coupled to the bus waveguide. The shape of the fabricated ring is noncircular to fit the resonator within one field of the electron-beam lithography tool and, hence, avoids stitching errors. VOA: Variable optical attenuator. M1, M2: Mirrors. BS: Beam splitter.

($n_2 = 2.5 \times 10^{-15}$ cm^2 W^{-1}, about 10 times that of silica) and very low propagation loss (< 0.5 dB cm^{-1}). It should be noted that the nonlinear refractive index of silicon is an order of magnitude higher than that of Si_3N_4, but nonlinear losses such as two-photon absorption and free-carrier absorption at 1550 nm prohibit parametric oscillation in silicon. The devices are compact, with a bus waveguide length of 1.5 mm and a ring circumference of 1.8 mm, corresponding to a free spectral range (FSR) of 80 GHz. In order to obtain FWM gain and optical parametric oscillation, the dispersion is engineered to be anomalous at the pump wavelength to compensate for the Kerr nonlinear phase shift due to the pump [26,30]. We design the ring waveguide cross section to be 820 nm high and 1700 nm wide, resulting in a slightly anomalous group-velocity dispersion at the pump wavelength of 1549.6 nm.

In order to obtain significant squeezing, the cavity output coupling losses must be a large fraction of the overall losses. Relatively large losses are also desired for a large cavity bandwidth. On the other hand, a low pump-power threshold is desirable, since it avoids detrimental thermal

effects and also minimizes the influence of technical noise from the pump laser. The squeezing factor depends on the ratio between the internal ring losses given by the ring's intrinsic quality factor (Q_i) and the coupling coefficient between the bus waveguide and the ring resonator determined by the loaded quality factor (Q_L). The smaller the ratio of these losses, the better the squeezing obtained. The squeezing factor relative to the shot-noise level can be quantified as [31–34]

$$S(\Omega) = 1 - \frac{\eta_c \eta_d}{1 + \Omega^2 \tau_c^2}, \qquad (1)$$

where Ω is the sideband frequency, τ_c is the cavity photon lifetime, η_d is the detection efficiency, and $\eta_c = 1 - Q_L/Q_i$ is the ratio of the coupling losses to the total losses.

The simultaneous requirement of large coupling losses and low threshold is a challenge, since the threshold is inversely proportional to the product of Q_i and Q_L. We can meet these requirements by designing a ring with a very large Q_i, larger than 2×10^6, and operating in the highly overcoupled regime. The high intrinsic Q achieved using the recently demonstrated fabrication process of thick Si_3N_4 deposition (Ref. [35]) enables the generation of the beams with a low-pump-power threshold of around 90 mW despite operating in this overcoupled regime. The corresponding intracavity power is estimated to be 7 W, which is an order of magnitude lower than the intracavity pump oscillation threshold of 65 W in Ref. [22]. The loaded Q (200 000) is designed to be much lower than the intrinsic Q ($Q_i \approx 2 \times 10^6$), facilitating a broad cavity linewidth of the order of 1 GHz.

The key to the realization of on-chip optical squeezing is the engineering of the dispersion and quality factors of the longitudinal modes of the microring resonator to generate the twin beams at two well-distinguished frequencies with low-threshold pump powers. In contrast to many tabletop squeezing experiments, where the twin beams can usually be separated spatially based on their different polarizations, in our platform the beams are copropagating in the same output waveguide with equal polarizations, and, therefore, in order to be distinguishable, the beams are required to have well-separated frequencies. A delicate interplay between the group-velocity dispersion and the quality factor of the ring, which together shape the FWM gain curve around the pump, determines at which frequencies the twin beams will be generated [34,36,37]. Specifically, the frequency difference between the pump and the first pair of oscillating signal and idler modes scales inversely as the square root of the second-order dispersion (D_2) and the loaded quality factor (Q_L): $\omega_{pump} - \omega_{signal} \propto FSR/\sqrt{Q_L D_2}$. Here we engineer the structure to ensure that the signal and the idler beams are generated at two well-distinguished wavelengths separated by around 20 nm, at 1540.2 and 1559.2 nm when the

OPO is pumped at 1549.6 nm, enabling the beams to be spatially separated using a diffraction grating with very low loss. These two modes are 15 cavity resonances away from the pump wavelength, as can be seen from the transmission spectrum of the ring shown in Fig. 1(b). The large wavelength separation between twin beams enables not only spatial separation of the twin beams but also enables filtering of the pump wavelength, which is essential to mitigate the effects of the residual pump from affecting the twin-beam squeezing measurements.

B. Device fabrication

The Si_3N_4 waveguides and ring resonators are fabricated in 820-nm-thick silicon nitride films to provide low loss and high optical confinement. A 4-μm-thick silicon dioxide layer is first thermally grown on a virgin silicon wafer as an undercladding. The nitride layer is grown using low-pressure chemical vapor deposition in two steps of 400 nm each, interleaved with annealing in a nitrogen atmosphere for 3 h at 1200 °C. The devices are patterned with electron-beam lithography using MaN-2403 as resist. After exposure and development, the resist is postexposure baked for 5 min. at 115 °C and etched in an inductively coupled plasma reactive ion etcher using CHF_3-O_2 chemistry. The devices are finally clad with 250 nm of high-temperature oxide deposited at 800 °C, followed by 2 μm of silicon dioxide using plasma-enhanced chemical vapor deposition. Further details about the fabrication process can be found in Ref. [35].

C. Experiment setup

The experiment setup used to measure the squeezing is shown in Fig. 2. The ring is pumped by a continuous-wave tunable laser (New Focus Velocity 6328) followed by an erbium-doped fiber amplifier (JDSU OAB1552 + 20FA6) and a BPF with a bandwidth of 9 nm to reduce the amplified spontaneous emission noise generated by the EDFA. Light is evanescently coupled to the microring through a waveguide. The output from the waveguide is collected with a high-NA (NA = 0.25) objective lens, leading to a loss of less than 1 dB. A diffraction grating with an efficiency of 85% is used to spatially separate the pump and the two beams. After blocking the pump, the beams are focused on the two inputs of a Thorlabs PDB 150C balanced detector. The balanced detection system consists of a pair of well-matched InGaAs photodiodes with a quantum efficiency of 80%, followed by a low-noise transimpedance amplifier to amplify the difference in photocurrents between the detectors. To observe the variance of the intensity-difference noise between the two balanced detectors, the rf output of the balanced detection system is sent to an electronic spectrum analyzer. The detection system has a bandwidth of 5 MHz and a transimpedance gain of 10^5 V/A. A small fraction (5%) of the light coming out of the chip is sent to an OSA to

observe the onset of parametric oscillation. The setup includes a VOA to calibrate the shot-noise level and to check the degradation of squeezing with attenuation of the twin beams.

III. RESULTS AND DISCUSSION

We measure the squeezing in intensity difference of the two beams generated when the triply resonant OPO is pumped above threshold by comparing the noise level to the shot-noise level generated from the coherent pump source.

A. Shot-noise calibration

We calibrate the shot-noise level by splitting the pump beam on a 50∶50 beam splitter, directing the two halves to the two detectors and monitoring the dc and ac components of the balanced detector output simultaneously. The common mode rejection ratio (CMRR) of the detectors is independently measured to be more than 27 dB. The laser is detuned far from the microring cavity resonance during shot-noise calibration measurements. The electronic noise of the detection system is measured by blocking all light incident on the detectors. As seen from Fig. 3, the detection system is linear over 20 dB near a sideband frequency of 3 MHz. There is excess technical noise at frequencies below 2 MHz, which cannot be rejected completely by the finite CMRR of the detection system. Focusing on the noise
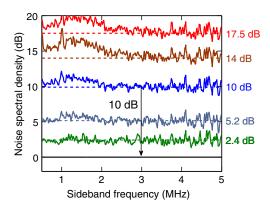

FIG. 3. Linearity of the balanced detection system from 0.5 to 5 MHz. The data are dark-noise corrected and normalized to the shot-noise spectrum at a base local oscillator (LO) power of $P_0 = 7.8 \, \mu$W, corresponding to the horizontal solid line at 0 dB. The dashed lines depict the mean optical power in the corresponding spectrum referenced to the base LO power P_0, in decibels. There is significant technical noise at low frequencies, which is clearly evident at relative powers above 10 dB. The data have more fluctuations at high frequencies due to higher electronic noise and consequently lower dark-noise clearance for the base LO power P_0. The dark noise varies from 5 dB below the 0-dB reference at 0.5 MHz to 1 dB below the reference at 5 MHz. Around 3 MHz, the detection system is linear over more than 20 dB, which is also substantiated by the linearity of the shot-noise calibration measurement in Fig. 4.

at 3 MHz, it can be seen from Fig. 4 that the shot-noise level is linearly proportional to the optical power in each beam, in accordance with theory.

B. Squeezing measurements

We observe more than 30% sub-shot-noise quantum intensity correlations between the twin beams generated when the pump laser is tuned to an on-chip resonance at 1549.6 nm. Twin-beam intensity-difference squeezing measurements are presented in Fig. 5(a). The solid line corresponds to the signal-idler intensity correlation measurement, which is below the shot-noise level, demonstrating clear intensity-difference squeezing. These measurements are taken at Fourier sideband frequencies from 0.5 to 5 MHz, using a spectrum analyzer with a resolution bandwidth of 30 kHz and a video bandwidth of 100 Hz. Squeezing is not observed at very low frequencies, owing to technical noise in the pump laser. The on-chip OPOs used here can, in principle, act as a platform for generating large squeezing factors over broad bandwidths due to the highly overcoupled design of the rings.

We confirm that the squeezing factor degrades linearly with increasing attenuation, and the intensity-difference noise approaches the shot-noise level for high attenuation, as is typical of squeezed states [Fig. 5(b)]. By using the VOA in the experiment setup (Fig. 2), we measure the influence of decreasing transmission through the VOA on the squeezed twin beams. The dependence of the variance of the intensity-difference noise normalized to the corresponding shot-noise level can be modeled by mixing the unattenuated two-mode squeezed state with a vacuum state on a beam splitter with transmittivity η:

$$\Delta^2 X_-(\eta) = \eta \Delta^2 X_-^{(0)} + (1 - \eta) \Delta^2 X_v, \quad (2)$$
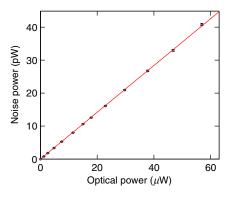

FIG. 4. Shot-noise calibration showing the linearity of the noise power in the photocurrent difference with optical power, as expected from theory. The data are taken at a Fourier sideband frequency of 3 MHz, using a spectrum analyzer with a resolution bandwidth of 30 kHz and a video bandwidth of 100 Hz. Data points are corrected by subtracting the electronic noise of the balanced detection system. Error bars are extracted from the raw data.
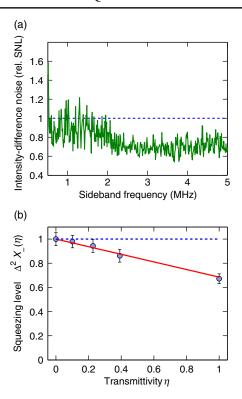
(a)

(b)

FIG. 5. Intensity-difference squeezing. (a) The variance of the signal and idler photocurrent difference normalized to the shot-noise level (SNL) on a linear scale. The dashed line at 1 represents the SNL, and the solid line represents the intensity-difference fluctuations. The dark-noise clearance is 16 dB at 0.5 MHz and decreases to 5 dB at 5 MHz. The data are taken with a pump power of 93 mW. The power in the signal and idler beams is 45 μW, which requires low-dark-noise detectors commercially unavailable at higher frequencies. Squeezing at low frequencies is masked by excess technical noise below approximately 2 MHz, that can be clearly seen in Fig. 3. (b) Variation of squeezing with attenuation at a sideband frequency of 3 MHz. The x axis is the transmittivity of the variable optical attenuator, η. The y axis is the intensity-difference noise in shot-noise units, that is, the variance of the signal and idler photocurrent difference compared to the shot-noise level. Error bars are determined from the standard deviation of the measured data points.

where the left-hand side represents the variance after attenuation, $\Delta^2 X_-^{(0)}$ represents the unattenuated variance (i.e., before the VOA), and $X_v = 1$ is the variance of vacuum. All variances are normalized to the shot-noise level at the corresponding power.

The observed noise reduction of 1.7 ± 0.4 dB corresponds to a generated squeezing of 5 dB when corrected for detection losses and the nonideal quantum efficiency of the detectors. This reduction is less than the 10 dB of squeezing expected from the ratio of Q_i and Q_L owing to residual excess pump noise of 25 dB relative to the shot-noise level and the possible rotation of the optimally squeezed quadratures by the process of FWM [38,39]. Furthermore, higher intrinsic quality factors of 7×10^6 have been demonstrated in silicon nitride rings [35], resulting in a

lower oscillation threshold, which helps not only in reducing excess noise in the pump but also leads to a higher ratio of Q_i to Q_L. It should, thus, be possible to reach much stronger noise reductions in this platform. Fundamentally, the on-chip OPOs are expected to exhibit squeezing over gigahertz bandwidths in view of the broad linewidth of the cavity. We demonstrate here squeezing in the megahertz range limited only by the bandwidth of our low-dark-noise detectors.

IV. CONCLUSIONS AND OUTLOOK

These results constitute an experimental demonstration of all-optical squeezing in an integrated CMOS-compatible platform. Our source generates bright squeezed light using a singly pumped FWM process, in contrast to other sources of above-threshold squeezing which utilize parametric down-conversion. Since FWM is based on the third-order nonlinearity, the technique presented here can be extended to several different material platforms, in contrast to the more restrictive second-order nonlinearity found only in noncentrosymmetric materials. For example, FWM oscillation has been reported in silica [40], crystalline fluorides [41], hydex [42], aluminum nitride [43], and diamond [44]. Our demonstration paves the way for a myriad of on-chip quantum-optics experiments over broad bandwidths in a scalable, compact, and robust platform. An experiment to measure phase anticorrelations of the twin beams is under way, enabling a demonstration of continuous-variable quantum entanglement [45]. This demonstration will open the way to realize deterministic quantum-information protocols at very high speeds. In the future, the frequency separation of the twin beams can be done on chip using ring-resonator-based add-drop filters tuned to the signal, idler, and pump wavelengths so that they are demultiplexed to different waveguides [46]. This integration opens up the possibility to cascade the on-chip OPO with photonic structures to manipulate squeezed and entangled states of light generated by the OPO, further emphasizing the highly scalable nature of our platform. The introduction of such nonclassical light sources into future data communications by leveraging the mature infrastructure of microelectronics, currently being introduced into silicon photonics [47], is a very promising avenue to be explored.

[1] K. Goda, O. Miyakawa, E. E. Mikhailov, S. Saraf, R. Adhikari, K. McKenzie, R. Ward, S. Vass, A. J. Weinstein, and N. Mavalvala, A quantum-enhanced prototype gravitational-wave detector, Nat. Phys. **4**, 472 (2008).

[2] LIGO Scientific Collaboration, A gravitational wave observatory operating beyond the quantum shot-noise limit, Nat. Phys. **7**, 962 (2011).

[3] E. S. Polzik, J. Carri, and H. J. Kimble, Spectroscopy with Squeezed Light, Phys. Rev. Lett. **68**, 3020 (1992).

[4] P. H. Souto Ribeiro, C. Schwob, A. Maître, and C. Fabre, Sub-shot-noise high-sensitivity spectroscopy with optical parametric oscillator twin beams, Opt. Lett. **22**, 1893 (1997).

[5] V. Giovannetti, S. Lloyd, and L. Maccone, Quantum-enhanced measurements: Beating the standard quantum limit, Science **306**, 1330 (2004).

[6] A. M. Marino and P. D. Lett, Absolute calibration of photodiodes with bright twin beams, J. Mod. Opt. **58**, 328 (2011).

[7] S. L. Braunstein and P. van Loock, Quantum information with continuous variables, Rev. Mod. Phys. **77**, 513 (2005).

[8] J. L. O'Brien, A. Furusawa, and J. Vučković, Photonic quantum technologies, Nat. Photonics **3**, 687 (2009).

[9] S. Clemmen, K. Phan Huy, W. Bogaerts, R. G. Baets, Ph. Emplit, and S. Massar, Continuous wave photon pair generation in silicon-on-insulator waveguides and ring resonators, Opt. Express **17**, 16558 (2009).

[10] J. E. Sharping, K. F. Lee, M. A. Foster, A. C. Turner, B. S. Schmidt, M. Lipson, A. L. Gaeta, and P. Kumar, Generation of correlated photons in nanoscale silicon waveguides, Opt. Express **14**, 12388 (2006).

[11] T. Suhara, Generation of quantum-entangled twin photons by waveguide nonlinear-optic devices, Laser Photonics Rev. **3**, 370 (2009).

[12] R. Horn, P. Abolghasem, B. J. Bijlani, D. Kang, A. S. Helmy, and G. Weihs, Monolithic Source of Photon Pairs, Phys. Rev. Lett. **108**, 153605 (2012).

[13] M. Davanco, J. R. Ong, A. B. Shehata, A. Tosi, I. Agha, S. Assefa, F. Xia, W. M. J. Green, S. Mookherjea, and K. Srinivasan, Telecommunications-band heralded single photons from a silicon nanophotonic chip, Appl. Phys. Lett. **100**, 261104 (2012).

[14] H. Takesue, H. Fukuda, T. Tsuchizawa, T. Watanabe, K. Yamada, Y. Tokura, and S.-i. Itabashi, Generation of polarization entangled photon pairs using silicon wire waveguide, Opt. Express **16**, 5721 (2008).

[15] F. Najafi, J. Mower, N. C. Harris, F. Bellei, A. Dane, C. Lee, X. Hu, P. Kharel, F. Marsili, S. Assefa, K. K. Berggren, and D. Englund, On-chip detection of non-classical light by scalable integration of single-photon detectors, Nat. Commun. **6**, 5873 (2015).

[16] A. I. Lvovsky, Squeezed light, arXiv:1401.4118.

[17] A. Heidmann, R. J. Horowicz, S. Reynaud, E. Giacobino, C. Fabre, and G. Camy, Observation of Quantum Noise Reduction on Twin Laser Beams, Phys. Rev. Lett. **59**, 2555 (1987).

[18] R. E. Slusher, L. W. Hollberg, B. Yurke, J. C. Mertz, and J. F. Valley, Observation of Squeezed States Generated by Four-Wave Mixing in an Optical Cavity, Phys. Rev. Lett. **55**, 2409 (1985).

[19] R. M. Shelby, M. D. Levenson, S. H. Perlmutter, R. G. DeVoe, and D. F. Walls, Broad-Band Parametric Deamplification of Quantum Noise in an Optical Fiber, Phys. Rev. Lett. **57**, 691 (1986).

[20] Ch. Silberhorn, N. Korolkova, and G. Leuchs, Quantum Key Distribution with Bright Entangled Beams, Phys. Rev. Lett. **88**, 167902 (2002).

[21] J. U. Fürst, D. V. Strekalov, D. Elser, A. Aiello, U. L. Andersen, Ch. Marquardt, and G. Leuchs, Quantum Light from a Whispering-Gallery-Mode Disk Resonator, Phys. Rev. Lett. **106**, 113901 (2011).

[22] S. Ast, M. Mehmet, and R. Schnabel, High-bandwidth squeezed light at 1550 nm from a compact monolithic PPKTP cavity, Opt. Express **21**, 13572 (2013).

[23] S. Ast, A. Samblowski, M. Mehmet, S. Steinlechner, T. Eberle, and R. Schnabel, Continuous-wave nonclassical light with gigahertz squeezing bandwidth, Opt. Lett. **37**, 2367 (2012).

[24] Y. Eto, A. Koshio, A. Ohshiro, J. Sakurai, K. Horie, T. Hirano, and M. Sasaki, Efficient homodyne measurement of picosecond squeezed pulses with pulse shaping technique, Opt. Lett. **36**, 4653 (2011).

[25] A. H. Safavi-Naeini, S. Gröblacher, J. T. Hill, J. Chan, M. Aspelmeyer, and O. Painter, Squeezed light from a silicon micromechanical resonator, Nature (London) **500**, 185 (2013).

[26] J. S. Levy, A. Gondarenko, M. A. Foster, A. C. Turner-Foster, A. L. Gaeta, and M. Lipson, CMOS-compatible multiple-wavelength oscillator for on-chip optical interconnects, Nat. Photonics **4**, 37 (2010).

[27] Y. Okawachi, K. Saha, J. S. Levy, Y. H. Wen, M. Lipson, and A. L. Gaeta, Octave-spanning frequency comb generation in a silicon nitride chip, Opt. Lett. **36**, 3398 (2011).

[28] M. A. Foster, J. S. Levy, O. Kuzucu, K. Saha, M. Lipson, and A. L. Gaeta, Silicon-based monolithic optical frequency comb source, Opt. Express **19**, 14233 (2011).

[29] V. R. Almeida, R. R. Panepucci, and M. Lipson, Nanotaper for compact mode conversion, Opt. Lett. **28**, 1302 (2003).

[30] A. C. Turner, C. Manolatou, B. S. Schmidt, M. Lipson, M. A. Foster, J. E. Sharping, and A. L. Gaeta, Tailored anomalous group-velocity dispersion in silicon channel waveguides, Opt. Express **14**, 4357 (2006).

[31] M. Brambilla, F. Castelli, L. A. Lugiato, F. Prati, and G. Strini, Nondegenerate four-wave mixing in a cavity: Instabilities and quantum noise reduction, Opt. Commun. **83**, 367 (1991).

[32] F. Castelli and P. Dotti, Quantum noise reduction in non-degenerate four-wave-mixing oscillators, Opt. Commun. **113,** 237 (1994).

[33] A. B. Matsko, A. A. Savchenkov, D. Strekalov, V. S. Ilchenko, and L. Maleki, Optical hyperparametric oscillations in a whispering-gallery-mode resonator: Threshold and phase diffusion, Phys. Rev. A **71,** 033804 (2005).

[34] Y. K. Chembo, Quantum correlations, entanglement, and squeezed states of light in Kerr optical frequency combs, arXiv:1412.5700.

[35] K. Luke, A. Dutt, C. B. Poitras, and M. Lipson, Overcoming Si_3N_4 film stress limitations for high quality factor ring resonators, Opt. Express **21,** 22829 (2013).

[36] M. R. E. Lamont, Y. Okawachi, and A. L. Gaeta, Route to stabilized ultrabroadband microresonator-based frequency combs, Opt. Lett. **38,** 3478 (2013).

[37] T. Herr, K. Hartinger, J. Riemensberger, C. Y. Wang, E. Gavartin, R. Holzwarth, M. L. Gorodetsky, and T. J. Kippenberg, Universal formation dynamics and noise of Kerr-frequency combs in microresonators, Nat. Photonics **6,** 480 (2012).

[38] C. J. McKinstrie and M. Karlsson, Schmidt decompositions of parametric processes I: Basic theory and simple examples, Opt. Express **21,** 1374 (2013).

[39] N. V. Corzo, Q. Glorieux, A. M. Marino, J. B. Clark, R. T. Glasser, and P. D. Lett, Rotation of the noise ellipse for squeezed vacuum light generated via four-wave mixing, Phys. Rev. A **88,** 043836 (2013).

[40] P. DelHaye, A. Schliesser, O. Arcizet, T. Wilken, R. Holzwarth, and T. J. Kippenberg, Optical frequency comb generation from a monolithic microresonator, Nature (London) **450,** 1214 (2007).

[41] A. A. Savchenkov, A. B. Matsko, V. S. Ilchenko, I. Solomatine, D. Seidel, and L. Maleki, Tunable Optical Frequency Comb with a Crystalline Whispering Gallery Mode Resonator, Phys. Rev. Lett. **101,** 093902 (2008).

[42] L. Razzari, D. Duchesne, M. Ferrera, R. Morandotti, S. Chu, B. E. Little, and D. J. Moss, CMOS-compatible integrated optical hyper-parametric oscillator, Nat. Photonics **4,** 41 (2010).

[43] H. Jung, C. Xiong, K. Y. Fong, X. Zhang, and H. X. Tang, Optical frequency comb generation from aluminum nitride microring resonator, Opt. Lett. **38,** 2810 (2013).

[44] B. J. M. Hausmann, I. Bulu, V. Venkataraman, P. Deotare, and M. Lončar, Diamond nonlinear photonics, Nat. Photonics **8,** 369 (2014).

[45] A. S. Villar, L. S. Cruz, K. N. Cassemiro, M. Martinelli, and P. Nussenzveig, Generation of Bright Two-Color Continuous Variable Entanglement, Phys. Rev. Lett. **95,** 243603 (2005).

[46] T. Barwicz, M. A. Popovic, P. T. Rakich, M. R. Watts, H. A. Haus, E. P. Ippen, and H. I. Smith, Microring-resonator-based add-drop filters in SiN: Fabrication and analysis, Opt. Express **12,** 1437 (2004).

[47] B. Jalali and S. Fathpour, Silicon photonics, J. Lightwave Technol. **24,** 4600 (2006).